

# Generation of 287 W, 5.5 ps pulses at 78 MHz repetition rate from a cryogenically cooled Yb:YAG amplifier seeded by a fiber chirped-pulse amplification system

Kyung-Han Hong,<sup>1,\*</sup> Aleem Siddiqui,<sup>1</sup> Jeffrey Moses,<sup>1</sup> Juliet Gopinath,<sup>2</sup> John Hybl,<sup>2</sup> F. Ömer Ilday,<sup>1</sup> Tso Yee Fan,<sup>2</sup> and Franz X. Kärtner<sup>1</sup>

<sup>1</sup>*Department of Electrical Engineering and Computer Science and Research Laboratory of Electronics, Massachusetts Institute of Technology, Cambridge, Massachusetts 02139, USA*

<sup>2</sup>*Massachusetts Institute of Technology Lincoln Laboratory, Lexington, Massachusetts 02420, USA*

\*Corresponding author: kyunghan@mit.edu

Received June 17, 2008; revised September 3, 2008; accepted September 8, 2008;  
posted September 23, 2008 (Doc. ID 97267); published October 23, 2008

We generate linearly polarized, 287 W average-power, 5.5 ps pulses using a cryogenically cooled Yb:YAG amplifier at a repetition rate of 78 MHz. An optical-to-optical efficiency of 41% is obtained at 700 W pump power. A 6 W, 0.4 nm bandwidth picosecond seed source at 1029 nm wavelength is constructed using a chirped-pulse fiber amplification chain based on chirped volume Bragg gratings. The combination of a fiber amplifier system and a cryogenically cooled Yb:YAG amplifier results in good spatial beam quality at large average power. Low nonlinear phase accumulation as small as  $5.1 \times 10^{-3}$  rad in the bulk Yb:YAG amplifier supports power scalability to a >10 kW level without being affected by self-phase modulation. This amplification system is well suited for pumping high-power high-repetition-rate optical parametric chirped-pulse amplifiers. © 2008 Optical Society of America

OCIS codes: 140.3280, 140.3615, 060.2320.

Optical parametric chirped-pulse amplification (OPCPA) [1] has been intensively investigated as an alternative method to chirped-pulse amplification (CPA), because it enables not only high-peak-power pulse generation but also ultrabroadband few-cycle pulse amplification at various wavelengths [2–4]. However, the requirements of a pump source for OPCPA are much more critical than those for the CPA technique, because parametric amplification with high efficiency while maintaining beam quality occurs only with a good spatiotemporal overlap between pump and seed beams. The development of a large-average-power picosecond pump source that can be synchronized with seed beams of either high or low repetition rate is one of the most important challenges. Besides the OPCPA applications, this laser source can be widely used for nonlinear frequency conversion to any desired wavelength range. Over the past several years, large-average-power high-repetition-rate picosecond laser technologies have been developed both on the basis of fiber and bulk amplifiers. On the side of fiber amplifier technologies, specifically based on ytterbium (Yb)-doped fibers, amplification of 10 ps pulses at 80 MHz to 51 W output power and at 47 MHz to 97 W output power has been demonstrated [5,6]. More recently, amplification of 20 ps pulses to 321 W output power was also reported [7]. In the latter case the repetition rate was as high as 1 GHz, significantly lowering the pulse energy, and for amplification to >100 W spectral broadening owing to self-phase modulation (SPM) was significant. Large-mode-area fiber technologies brought a great advance in femtosecond pulse amplification up to ~100 W average powers. On the side of bulk amplifier technologies, several solid-state picosecond

laser systems, based on Nd:YAG, thin-disk Yb:YAG, and Nd:YVO<sub>4</sub>, with average powers of up to 111 W have been demonstrated [8–10]. Bulk amplifiers still have more feasibility in terms of power scaling and polarization maintenance than fiber amplifiers owing to the large cross section, high doping rate, and short length of gain materials. Recently, a cryogenically cooled Yb:YAG laser has proven to be a good candidate for the average power scaling because of its good thermo-optic properties, small quantum defect, and low saturation fluence (2 J/cm<sup>2</sup> at 70 K). At cryogenic temperatures Yb:YAG has an emission bandwidth of 1.5 nm, making it compatible with picosecond pulse amplification. Based on the cryogenic-cooling technique, a high-power cw Yb:YAG laser system with >450 W has been already demonstrated [11]. Amplifiers for picosecond pulses at 10 Hz with 7 mJ [12] and at tens of kilohertz with an average power of 24 W [13] have also been demonstrated.

In this Letter, we report on direct amplification of 5.5 ps pulses with a cryogenically cooled Yb:YAG amplifier at 78 MHz reaching 287 W of average power. To our knowledge, this is the highest average-power picosecond pulse train at the megahertz repetition rate. The amplified pulses have a spectral bandwidth of 0.3 nm centered at 1029 nm and good beam quality. We also describe a 6 W picosecond fiber CPA system based on chirped volume Bragg gratings (CVBGs) [14] as a picosecond seed source for the Yb:YAG amplifier.

Figure 1 illustrates the optical layout of the fiber CPA chain and the cryogenically cooled Yb:YAG amplifier. As a master oscillator at 78 MHz, we used a femtosecond Yb-doped fiber laser with an output power of 58 mW and a spectral bandwidth of ~50 nm

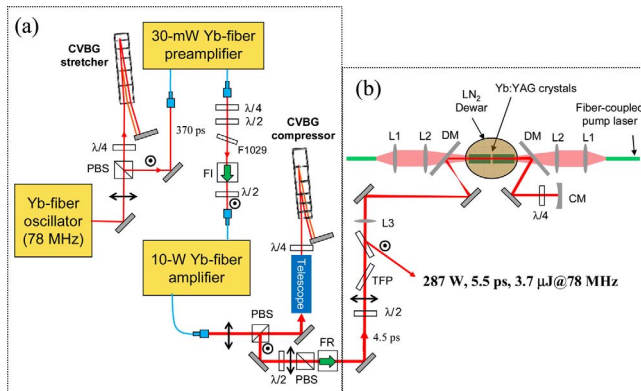


Fig. 1. (Color online) Optical layout of a high-average-power picosecond laser system: (a) 6 W fiber CPA chain and (b) 287 W cryogenically cooled double-pass Yb:YAG amplifier. PBS, polarization beamsplitter;  $\lambda/4$ , quarter-waveplate;  $\lambda/2$ , half-wave-plate; F1029, narrow bandpass filter at 1029 nm; FI, Faraday isolator; FR, Faraday rotator; CVBG, chirped volume Bragg grating; TFP, thin-film polarizer; L1,  $f=50$  mm lens; L2,  $f=200$  mm lens; L3,  $f=500$  mm lens; CM, radius of curvature=1000 mm concave mirror; DM, dichroic mirror.

centered at 1030 nm. The use of a femtosecond laser as a seed source for a picosecond amplifier allows wavelength matching to various  $1 \mu\text{m}$  amplifier media, as demonstrated with self-synchronized OPCPA systems seeded by a broadband Ti:sapphire laser [2,4]. The narrowband 1029 nm portion was selectively amplified in the fiber CPA chain, as explained below. The two-stage Yb-doped fiber amplifier shown in Fig. 1(a) is comprised of a single-mode preamplifier and a 10 W polarization-maintaining amplifier (YAR-15k-1064, IPG Photonics). Direct amplification of the unchirped seed pulses after simple spectral filtering leads to strong SPM and limited the amplification to only  $\sim 0.3$  W. The fiber-core diameter of  $12 \mu\text{m}$  of the 10 W amplifier limits the output peak power to  $\sim 1$  kW before strong SPM occurs. However, several watts of seed power within the required narrow spectral bandwidth of 1.5 nm are necessary for efficient amplification in the cryogenic Yb:YAG amplifier. To boost the average power without SPM in the fiber amplifier, we employed a compact CPA technique based on CVBGs that enable the stretching of a narrowband picosecond pulse to  $>100$  ps and recompression to the original pulse duration at high efficiency [14]. A CVBG can be regarded as a bulk version of a chirped fiber Bragg grating or a picosecond version of a chirped mirror with an extreme thickness. The CVBGs (OptiGrate, Inc.) support a narrow bandwidth of 2.2 nm centered at 1036 nm, but the wavelength can be tuned to 1029 nm by variation of the incident angle by  $\sim 9^\circ$  and by using a double-pass scheme. They have a cross section of  $5.0 \text{ mm} \times 4.4 \text{ mm}$  and a thickness of 23 mm. The stretched pulse duration after the double pass was measured to be  $\sim 370$  ps with a sampling scope and 10 GHz photodetector. The 0.8 mW stretched pulse was amplified to 30 mW by the preamplifier and then launched into the 10 W amplifier at 8 mW using a free-space-to-fiber coupler. Polarization control and isolation was

achieved using quarter- and half-wave-plates and a Faraday isolator [ $\lambda/4$ ,  $\lambda/2$ , and FI in Fig. 1(a)]. A narrowband (3.5 nm) interference filter at 1029 nm separates the 976 nm pump beam powering the preamplifier. We obtained a maximum average power of 10.8 W from the two-stage fiber amplifier chain and then compressed the output pulses to 4.5 ps with a bandwidth of 0.4 nm. The amplified spectrum is free of SPM-induced spectral broadening down to  $-50$  dB, limited by the measurement only. It should be noted, however, that the current CVBGs incur nonnegligible spatial chirp owing to some tilt of the chirped index distribution in the CVBGs. The spectral filtering effect owing to the spatial chirp at the free-space-to-fiber coupling optics and gain narrowing effects reduced the amplified bandwidth to 0.4 nm. The compressed power was 6.0 W at 10.8 W from the amplifier, corresponding to a compression efficiency of 56%. The focused spot from the CVBG compressor showed an elliptical shape (ellipticity of  $\sim 0.5$ ) owing to the spatial chirp even though the near-field pattern was still nearly Gaussian. The same feature of the further amplified beam will be discussed in Fig. 4. Nevertheless, this fiber CPA system generated narrow-bandwidth picosecond pulses with enough average power and good beam quality to seed the cryogenic Yb:YAG amplifier.

The 6 W, 4.5 ps pulse train generated in the fiber CPA system was delivered to the cryogenically cooled two-pass Yb:YAG amplifier pumped by 700 W of power from two fiber-coupled laser diodes, as illustrated in Fig. 1(b). The actual seed power arriving at the Yb:YAG crystal was  $\sim 4$  W owing to power degradation in the fiber amplifier and loss in the polarization optics [TFP, FR, and PBS in Fig. 1(b)]. The 940 nm pump beams, delivered by two 0.4 mm diameter multimode fibers, are focused at each of two crystals to a diameter of  $\sim 1.6$  mm using an  $f=50$  mm collimator (L1) and an  $f=200$  mm lens (L2). Both 23 mm long Yb:YAG crystals with normal cut and antireflection coating have a doping concentration of 2 at. % and a 1 mm undoped YAG endcap on the sides where the pump beams enter. They are cryogenically cooled to 77 K by liquid nitrogen in

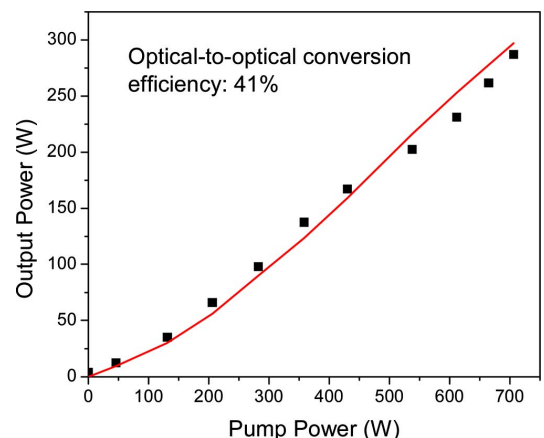


Fig. 2. (Color online) Average output power versus pump power. Squares represent the measured values, while the solid curve shows the calculated curve.

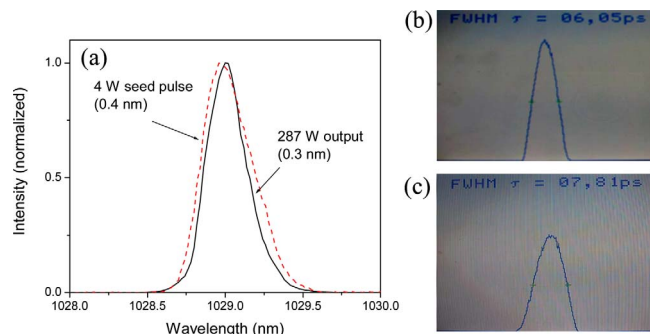


Fig. 3. (Color online) Optical spectra of input pulse (dashed curve) and amplified pulse (solid curve) at (a) Yb:YAG amplifier and (b) raw image of autocorrelation traces of input pulse and (c) amplified pulse. Corresponding pulse durations for (b) and (c) are 4.5 and 5.5 ps, respectively.

vacuum. The double-pass geometry was implemented using two thin-film polarizers and a quarter-waveplate, ensuring the linearly polarized output pulses. The  $\sim 3$  mm diameter of seed beam size was reduced to  $< 1.5$  mm at the crystal using a lens (L3) in a near-field plane. The beam size at the second pass was also kept to a similar size using a concave mirror (CM) located at a confocal position to L3. Figure 2 shows the measured and calculated output powers versus pump power. We obtained an average output power as high as 287 W with 700 W of pump power with an optical-to-optical efficiency of 41%. The calculated output power versus pump power, assuming a Gaussian beam profile and taking into account temperature effects and loss owing to amplified spontaneous emission, shows good agreement for the entire range of pump power as seen in Fig. 2. The slope efficiency was also 41%. The measured spectra before and after the amplification with the cryogenic Yb:YAG amplifier are shown as solid and dashed curves, respectively, in Fig. 3(a), while the corresponding autocorrelation traces are also shown in Figs. 3(b) and 3(c). The amplified pulse duration was 5.5 ps (FWHM) from the autocorrelation trace of Fig. 3(c), which is only 1.4 times the transform-limited pulse duration. Considering the estimated  $B$ -integral value of only  $5.1 \times 10^{-3}$  rad at the Yb:YAG crystals, the average power could be potentially scaled to  $> 10$  kW without being limited by SPM. Finally, we also characterized

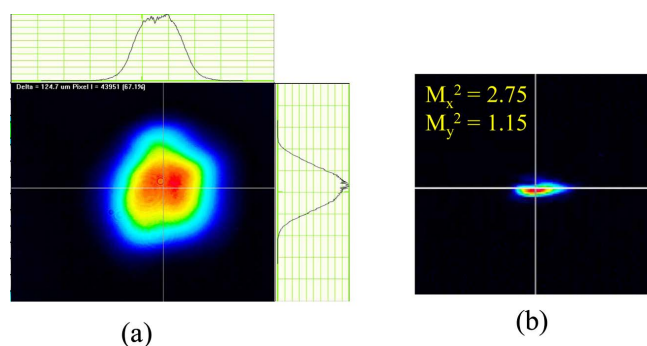


Fig. 4. (Color online) (a) Near-field and (b) far-field patterns of amplified beam. Measured  $M^2$  values are 2.75 in the horizontal and 1.15 in the vertical directions.

the spatial properties of the amplified pulses. Figures 4(a) and 4(b) show the near- and far-field images of the beam, respectively. The far-field image reveals an elliptical focused spot owing to the spatial chirp induced by the CVBG, resulting in a  $M^2$  of 2.75 in the horizontal direction, whereas the  $M^2$  in the vertical direction was only 1.15, almost diffraction limited. In fact, the direction of the spatial chirp is rotatable depending on the CVBG installation angle, indicating that the nonideal beam quality originates from the nonoptimal fabrication of the CVBGs. In addition, further calculation shows that the spatial optimization of seed and pump beams can enhance the optical efficiency to  $> 50\%$  or the average power to  $> 350$  W.

This work was supported by the U.S. Air Force Office of Scientific Research (AFOSR) (FA9550-06-1-0468 and FA9550-07-1-0014) through the Defense Advanced Research Projects Agency (DARPA) Hyperspectral Radiography Sources program and MIT Lincoln Laboratory.

## References

1. A. Dubietis, R. Butkus, and A. Piskarskas, *IEEE J. Sel. Top. Quantum Electron.* **12**, 163 (2006).
2. T. Fuji, N. Ishii, C. Y. Teisset, X. Gu, Th. Metzger, A. Baltuska, N. Forget, D. Kaplan, A. Galvanauskas, and F. Krausz, *Opt. Lett.* **31**, 1103 (2006).
3. G. Cirmi, D. Brida, C. Manzoni, M. Marangoni, S. De Silvestri, and G. Cerullo, *Opt. Lett.* **32**, 2396 (2007).
4. J. Moses, O. D. Mücke, A. Benedick, E. L. Falcão-Filho, S.-W. Huang, K.-H. Hong, A. M. Siddiqui, J. R. Birge, F. Ö. Ilday, and F. X. Kärtner, presented at the Conference on Lasers and Electro-Optics and Quantum Electronics and Laser Science (CLEO/QELS 2008), San Jose, May 4–9, 2008, paper CTuEE2.
5. J. Limpert, A. Liem, T. Gabler, H. Zellmer, A. Tünnermann, S. Unger, S. Jetschke, and H.-R. Müller, *Opt. Lett.* **26**, 1849 (2001).
6. J. Limpert, N. Deguil-Robin, I. Manek-Hönninger, F. Salin, T. Schreiber, A. Liem, F. Roser, H. Zellmer, A. Tünnermann, A. Courjaud, C. Hönninger, and E. Mottay, *Opt. Lett.* **30**, 714 (2005).
7. P. Dupriez, A. Piper, A. Malinowski, J. K. Sahu, M. Ibsen, B. C. Thomsen, Y. Jeong, L. M. B. Hickey, and M. N. Zervas, *IEEE Photon. Technol. Lett.* **18**, 1013 (2006).
8. G. J. Spühler, T. Südmeyer, R. Paschotta, M. Moser, K. J. Weingarten, and U. Keller, *Appl. Phys. B* **71**, 19 (2000).
9. F. Brunner, E. Innerhofer, S. V. Marchese, T. Südmeyer, R. Paschotta, T. Usami, H. Ito, S. Kurimura, K. Kitamura, G. Arisholm, and U. Keller, *Opt. Lett.* **29**, 1921 (2004).
10. L. McDonagh, R. Wallenstein, and A. Nebel, *Opt. Lett.* **32**, 1259 (2007).
11. T. Y. Fan, D. J. Ripin, R. L. Aggarwal, J. R. Ochoa, B. Chann, M. Tilleman, and J. Spitzberg, *IEEE J. Sel. Top. Quantum Electron.* **13**, 448 (2007).
12. Y. Akahane, M. Aoyama, K. Ogawa, K. Tsuji, S. Tokita, J. Kawanaka, H. Nishioka, and K. Yamakawa, *Opt. Lett.* **32**, 1899 (2007).
13. S. Tokita, J. Kawanaka, Y. Izawa, M. Fujita, and T. Kawashima, *Opt. Express* **15**, 3955 (2007).
14. K.-H. Liao, M.-Y. Cheng, E. Flecher, V. I. Smirnov, L. B. Glebov, and A. Galvanauskas, *Opt. Express* **15**, 4876 (2007).